Published in final edited form as:
Nat Genet. 2015 October ; 47(10): 1158–1167. doi:10.1038/ng.3381.

Absence of canonical active chromatin marks in developmentally regulated genes

Sílvia Pérez-Lluch[#1,2,3,4], **Enrique Blanco**[#1,3,4], **Hagen Tilgner**[#1,2,5], **Joao Curado**[#1,2,6], **Marina Ruiz-Romero**[3,4], **Montserrat Corominas**[3,4], and **Roderic Guigó**[1,2]

[1]Centre for Genomic Regulation. Barcelona, Catalonia, Spain.

[2]Universitat Pompeu Fabra. Barcelona, Catalonia, Spain.

[3]Departament de Genètica (Facultat de Biologia) , Universitat de Barcelona. Barcelona, Catalonia, Spain.

[4]Institut de Biomedicina de la Universitat de Barcelona. Barcelona, Catalonia, Spain.

[6]Graduate Program in Areas of Basic and Applied Biology, Abel Salazar Biomedical Sciences Institute, University of Porto, Porto, Portugal.

[#] These authors contributed equally to this work.

Abstract

The interplay of active and repressive histone modifications is assumed to play a key role in the regulation of gene expression. In contrast to this generally accepted view, we show that transcription of genes temporally regulated during fly and worm development occurs in the absence of canonically active histone modifications. Conversely, strong chromatin marking is related to transcriptional and post-transcriptional stability, an association that we also observe in mammals. Our results support a model in which chromatin marking is associated to stable production of RNA, while unmarked chromatin would permit rapid gene activation and de-activation during development. In this case, regulation by transcription factors would play a comparatively more important regulatory role.

Post-translational modifications of histones define an evolutionarily conserved “code” that governs differential gene expression[1]. Trimethylation of histone H3 at lysine 4 (H3K4me3) and at lysine 36 (H3K36me3), for instance, correlate with active transcription, whereas H3K9me3 and H3K27me3 are usually linked to transcriptional repression[2, 3]. The

Corresponding authors: Montserrat Corominas (mcorominas@ub.edu) and Roderic Guigó (roderic.guigo@crg.cat).
[5]Present address: Department of Genetics, Stanford University, Stanford, California, USA.

Author contributions

S. P-Ll. and M. R-R performed the experiments, E. B., H. T. and J. C. performed the computational analyses; M. C. and R. G designed the study and wrote the manuscript with contributions from all authors.

Accession codes

ChIPSeq and RNASeq raw data and profiles of read counts were deposited in the NCBI-GEO repository under the accession number GSE56551.

Competing financial interests

The authors declare no competing financial interests.

Europe PMC Funders Author Manuscripts

combinatorial behavior of histone modifications along regulatory regions—reflecting and/or influencing the specific arrangement of transcription factors—modulates the expression levels of genes, conferring them with a unique temporal and spatial transcriptional program. Computational models have been developed that can predict gene expression from histone modifications with great accuracy[4, 5].

A number of recent reports, however, indicate that expression of certain genes may occur in absence of histone modifications canonically associated to active genes. The modENCODE project reported that some expressed genes lacked H3K4me3[6]. Hödl and Basler found that cells that lack H3K4 methylation, respond to developmental signaling pathways by activating target gene expression in *Drosophila* wing imaginal discs[7]. Chen et al. observed that pre-midblastula transition (pre-MBT) genes have particularly low levels of H3K4me3[8]. More recently, Zhang et al. reported that genes within yeast heterochromatic regions can be transcribed in absence of active histone marks[9]. Here, we show that active transcription in the absence of chromatin marking is actually a general feature of genes that are strongly regulated during development. We analyzed data produced by modENCODE in whole animals and tissues in fly and worm, characterized the fly transcriptome by RNASeq and the epigenome by ChIPSeq in two spatially well-defined and relatively homogeneous developmental fly tissues, and carried out targeted experimental validations in isolated cells. All these analyses strongly suggest that expression of genes regulated during fly development can occur in the absence of marks typically associated with active genes, and, indeed, this expression does not seem to be affected by perturbations of the histone methyltransferase system. Conversely, we found that chromatin marking is associated not only to transcriptional levels, but also to transcriptional and post-transcriptional stability—an association that appears to be conserved through metazoan evolution.

Results

Expression without histone modifications during development

To investigate the dynamics of chromatin marking in genes regulated during development, we analyzed data produced within the *Drosophila melanogaster* modENCODE project[6, 10]. We specifically analyzed RNASeq and ChIPSeq data for H3K4me3, H3K9ac, H3K4me1, H3K27ac, H3K27me3 and H3K9me3 on whole animals (Supplementary Fig. 1a). To measure transcriptional stability, we computed the coefficient of variation of gene expression over 12 developmental time points (Methods and Supplementary Fig. 1b)—lower values corresponding to higher transcriptional stability. The distribution of the coefficient of variation uncovers a large class of genes that show constant expression during development, and two other minor classes containing genes whose expression is highly variable—often restricted to a limited number of stages (Supplementary Fig. 1c, d). We arbitrarily selected the 1,000 genes with the highest coefficient of variation, and defined them as developmentally regulated, because of their variable pattern of expression along time. Conversely, we selected the 1,000 genes with the lowest coefficient of variation, and defined them as developmentally stable. For each gene, we determined the time point at which its expression is the highest. At this time point, we did not observe strong differences between the expression of stable and regulated genes (Fig. 1a). At the same time point we measured

the levels of histone modifications for each gene (Methods). We found that at the point of highest expression, stable genes are strongly marked by histone modifications typically associated to active transcription, H3K4me3 and H3K9ac, and also to enhancers: H3K4me1 and H3K27ac. Unexpectedly, however, regulated genes show very low levels of these modifications, comparable to those of silent genes (Fig. 1b, Supplementary Fig. 2). In Figure 1c we compare the pattern of H3K4me3 along fly development in *CG8636*, a gene stably expressed during development, and in *CG16733,* a gene specifically expressed in pupa. *CG8636* shows a strong H3K4me3 peak downstream from the transcription start site whereas *CG16733* lacks any marking, even at the pupa stage, where it is expressed at higher levels than *CG8636*. (See also Supplementary Fig 3.) This contrasting pattern of histone marking is not only apparent when comparing genes with extreme behavior, but it is a distinct feature of the partition of the entire set of fly genes in two major classes according to transcriptional stability (Supplementary Fig. 4). For the histone modifications typically associated to inactive genes, H3K27me3 and H3K9me3, we observed that regulated genes showed levels higher than those of stable ones, and similar to those of silent genes (Methods, Fig. 1d). The levels of these marks, however, are generally low compared to the levels of active marks, even for genes silent during development—a large proportion of which lack any evidence of them (Supplementary Fig. 5a, b), as it has already been previously reported[11]. We found only a weak relationship between the level of repressive marks and gene expression (Supplementary Fig. 5c, d).

Given that developmental chromatin maps produced in the modENCODE project are on whole organisms, it could be argued that apparent lack of chromatin marking is the consequence of the expression of regulated genes being spatially confined to specific organs, tissues or subtissular domains. While, indeed, regulated genes show in general a spatially restricted pattern of expression, chromatin marking can actually be detected in stable genes that exhibit also a restricted expression pattern comparable to that in regulated genes (Supplementary Fig. 3). To further investigate the potential effect of restricted expression in the ability to detect chromatin marking, we used tissue-specific RNASeq data from modENCODE[12]. Third instar larva (L3) is the time point with the largest number of tissues available: carcass, central nervous system, digestive system, fat body, imaginal discs and salivary glands. Using L3 tissue-specific RNASeq data, we identified seven regulated genes expressed in all six available tissues at L3 (“Regulated broadly-expressed” Fig. 2a, left panel). Conversely, we identified 130 stable genes specifically expressed in only one of the aforementioned tissues in L3 (“Stable tissue-specific”, Fig. 2a, right panel). Regulated broadly-expressed genes have much higher expression levels than stable tissue-specific genes when measured in the whole body (almost four-fold, Fig. 2b), as well as, in general, when measured on individual tissues (Supplementary Fig. 6). They have also higher expression levels than stable genes overall. However, the levels of H3K4me3, H3K9ac, H3K4me1, and H3K27ac in regulated broadly-expressed genes are significantly lower than in stable genes, even than in stable tissue-specific genes, and comparable to those in silent genes (Fig. 2c). We confirmed both gene expression and levels of H3K4me3 and H3K9ac by qPCR (Fig. 2b) and ChIP-qPCR (Fig. 2d), respectively.

All these results strongly suggest that activation of genes regulated during development occurs mostly in the absence of histone modifications canonically linked to active genes.

Our results also point to strong chromatin marking association not only with transcriptional levels, but also with transcriptional stability. We calculated the coefficient of correlation (cc) across all genes between the coefficient of variation of gene expression across developmental time points as computed above, and the level of histone modifications at the developmental time point of highest expression. We used partial correlations to control for a potential confounding effect of gene expression levels (see Methods). For all active histone modifications, the partial correlations are negative and significant (as low as cc = −0.68 for H3K4me3, Fig. 3a, b, Supplementary Fig. 7), strongly supporting association between transcriptional stability and active chromatin marking.

To investigate whether lack of chromatin marking in regulated genes and the association between chromatin marking and transcriptional stability are conserved in other metazoans, we first analyzed RNASeq-based gene expression on seven time points through *C. elegans* development[13] and ChIP-chip data on two histone modifications available for these time points in modENCODE: H3K4me3 and H3K36me3. While both, the resolution and the reliability of the chromatin data obtained through ChIP-chip are lower in worm than in the fly ChIPSeq, we observed the same trend: the expression level at the time point of maximum expression is very similar in regulated and stable genes (Fig. 3c), while regulated genes show lower levels of H3K4me3 and H3K36me3, more similar to those of silent genes (Fig. 3d). As in flies, there is a significant association between transcriptional stability and active histone marking (Fig. 3b).

Unfortunately, genome-wide transcriptomic and epigenetic developmental maps of the resolution of those from modENCODE are not yet available for mammalian (or vertebrate) systems. Nevertheless, using transcriptomic and epigenomic data across multiple tissues and cell lines in human and mouse, we did find that active chromatin marking is associated to transcription stability also in mammalian systems. We used RNASeq and ChIPSeq data for H3K4me3, H3K36me3 and H3K4me1 for 56 human adult and fetal tissues, primary cells and cultured cell lines from the Roadmap Epigenomics Mapping Consortium[14]. We found strong negative correlation between the coefficient of variation of gene expression across these samples, and histone levels (Fig. 3b). The gene set with highest variation of expression across human tissues is likely to show some enrichment in regulated genes. Thus, we selected the 1,000 genes with the highest coefficient of variation as variably expressed genes, and the 1,000 genes with the lowest as constantly expressed. In the cell type in which the expression of each gene is highest, variable genes show higher expression than constant genes (Figure 3e). Yet, the levels of active histone modifications in these cell types are much lower in variable than in constant genes (Fig. 3f, Supplementary Fig. 8a). Very similar results are obtained in mouse when using ENCODE data[15] (Fig. 3b, g, h and Supplementary Fig. 8b).

Expression without histone modifications in imaginal discs

Data generated by the modENCODE projects monitor complex systems encapsulating great cellular heterogeneity. To investigate the dynamics of chromatin marking during development in a more homogeneous cellular environment, we characterized the transcriptome by RNASeq (Supplementary Fig. 9a, b and Supplementary Table 1) and the

epigenome by ChIPSeq in two *D. melanogaster* third instar larval tissues: Wing and Eye-antenna imaginal discs (WID and EID, respectively). We specifically monitored H3 and the active marks H3K4me3, H3K9ac, H3K4me1, and H3K27ac, plus the transcription elongation mark H3K36me3 (Supplementary Fig. 9c). Both, WID and EID, are epithelial tissues in early differentiation stages, and differentially expressed genes are likely to be under temporal developmental control. While WID and EID epigenomes and transcriptomes are very similar (Supplementary Fig. 9d-e), differentially expressed genes do exhibit functions strongly consistent with the known biology of these tissues (Supplementary Tables 2, 3 and Supplementary Fig. 9f).

We then investigated the marking of regulated and stable genes in WID and EID. To focus on genes under stronger regulation, we identified 55 developmentally regulated genes expressed in EID, but not in WID, and 10 regulated genes expressed in WID, but not in EID. We also identified a set of 284 stable genes highly expressed both in EID and WID, as well as a set of 30 genes silent in both (Supplementary Tables 4-7 and Methods).

We next compared marking of stable, silent, and regulated WID- and EID-specific genes (from now on simply, WID- and EID-specific). Consistent with previous observations[16, 17], the WID- and EID-profiles of stable genes are very similar, as are those of silent genes (Fig. 4a). Stable and silent genes are both characterized by higher stable nucleosome occupancy than nearby intergenic regions, but the genic nucleosome (H3) enrichment is larger for stably expressed than for silent genes. Stable genes are also strongly marked by H3K4me3, H3K9ac, H3K36me3, and also, as observed in modENCODE, by H3K4me1 and H3K27ac. Silent genes mostly lack these histone modifications. Regulated tissue-specific genes exhibit, however, a contrasting behavior. As expected, WID-specific genes lack active modifications in EID (Fig. 4b), and, conversely, EID-specific genes are not marked in WID (Fig. 4c). Unexpectedly, but consistently with the behavior that we observed in modENCODE data, WID-specific genes are not marked in WID either, nor EID-specific genes in EID. Absence of active histone marking cannot be attributed to the lack of nucleosomes because H3 is observed in these genes (Fig. 4b, c). It is unlikely that it originates either from higher nucleosome turnover in regulated genes since, at least in *Drosophila* S2 cells[18], nuclear turnover is similar for stable and regulated genes (Supplementary Fig. 10). Lack of histone marking is not due, either, to the relative low expression level of WID- or EID-specific genes, since even when these genes have high levels of expression, comparable to those of constitutively expressed genes, there is no marking by active modifications. This is illustrated in Figure 5 (see Supplementary Fig. 11 for more examples). The WID-specific gene *CG4382* and the EID-specific gene *CG14516* have similar levels of expression than the stable gene *noc*. This gene, however, is strongly marked by histone modifications in both WID and EID, while *CG4382* and *CG14516* are marked in neither. Lack of chromatin marking cannot be attributed to the restricted expression of tissue-specific genes, since the expression of *noc* is also restricted to specific regions both in WID and EID[19, 20]. H3 levels of tissue-specific and stable genes are comparable and only depend weakly on the expression status of genes (Fig. 5).

Active transcription without histone modifications

While WID and EID are relatively homogeneous tissues, they already show cellular sub-specialization at third instar larvae. For instance, the WID-specific gene *POU domain protein 2* (*pdm2*), like *nubbin* (*nub*)[21], with strong temporal and spatial regulation during development, is only expressed in the wing primordium (wing pouch) at third instar larva (Fig. 6a). To unequivocally demonstrate lack of chromatin marking in developmentally regulated genes, we took advantage of the *nub*-GAL4 construct to drive expression of GFP only in the wing pouch, where *pdm2* is expressed. Thus, we collected all cells expressing *pdm2* and investigated chromatin marking for this gene only in the cells in which it is expressed. More specifically, dissection and dissociation of wing discs followed by cell-sorting analyses allowed the isolation of two populations of cells: the wing pouch (*nub* domain, GFP positive) and the rest of the wing (GFP negative) (Fig. 6a and Methods). By using qPCR we found that the expression of *pdm2*, restricted to sorted GFP positive cells, is even higher than the expression of *crm*, a gene expressed at the same level throughout the WID (Fig. 6b). ChIP assays followed by qPCR on sorted cells showed that the levels of H3K4me3, and H3K36me3 in *pdm2* are significantly lower than in *crm*, and comparable to those in *CG10013,* a gene silent in the whole WID (Fig. 6c). High RNA levels of *pdm2* in the wing pouch (Fig. 6b) do not necessarily demonstrate active transcription, since transcription could have occurred at an earlier time point. To assess active gene expression we directly measured newly transcribed RNA (nascent RNA) in sorted cells. As shown in Figure 6d, *pdm2* active transcription in GFP positive cells is as high as transcription of the control gene *crm*.

To investigate marking by repressive histone modifications in expressed genes (Fig 1d), we monitored the levels of H3K27me3 in *pdm2*, a gene exhibiting this modification at L3 when measured in the whole organism. We performed individual ChIP-qPCR in sorted cells and found that *pdm2* is indeed marked by H3K27me3 in WID, but only outside the wing pouch. No marking was observed in the wing pouch, where *pdm2* is expressed (Fig. 6e). This suggests that the repressive modifications detected in whole organisms in regulated genes (Fig. 1d) could originate from organs or tissues in which these genes are not expressed.

Lack of active marking suggests that genes regulated throughout development may not respond to histone modification systems. Therefore, we specifically investigated the response of regulated genes to the lack of ASH2 (*Absent, small or homeotic disc 2*), a key co-factor for H3K4 methylation[22]. First we characterized ASH2 occupancy along fly genes using ChIPSeq data obtained in WID[17] and found a very strong depletion of ASH2 binding to the promoters of regulated genes compared to those of stable genes (Fig. 7a). Second, we used the $ash2^{I1}$ mutant allele to interfere with H3K4me3. Since this allele is lethal in late third-instar larvae/early pupae[23], we performed clonal analyses in WID and EID. We specifically analyzed two stable genes: *engrailed* (e*n*), expressed in the posterior compartment of the WID, and *Cyclin A* (*CycA*), ubiquitously expressed in the WID, as well as two regulated genes: *pdm2*, expressed in the wing pouch, and *bride of sevenless* (*boss*), expressed in the differentiated photoreceptor R8 cell of the EID. We confirmed lack of H3K4me3 in $ash2^{I1}$mutant clones (Fig. 7b), and observed a clear reduction in the levels of En and CycA, while the expression of Boss and *pdm2* was not affected (Fig. 7c-p).

Genome organization of regulated genes

It has been suggested that developmental control genes are under a characteristic regulatory program[24]. They tend to harbor increased number of transcription factor binding sites[25] and are characterized by "peaked" (or narrow) promoters, compared to housekeeping genes which are associated to more "dispersed" (or broad) promoters[26-29]. Using the promoter classification of Ni et al.[30], we found that stable genes are strongly enriched in broad (and weak) promoters compared to regulated genes (444 vs. 12). In contrast, the proportion of peaked promoters is similar in stable and regulated genes (42 vs. 38). Overall, however, our set of regulated genes exhibits most of the characteristics that have been reported for developmental and/or peaked promoter genes in *Drosophila* and other species (see Lenhard et al.[31] for a review). Thus, promoters of regulated genes show stronger conservation[29-31], particularly in predicted transcription factor binding motifs (Supplementary Fig. 12). They are depleted in DNA Replication related Element (DRE) sequences, which are associated to disperse initiation of transcription[8] (15% of regulated compared to 39% of stable genes), and enriched in TATA Binding Protein (TBP) boxes, characteristic of tighter gene regulation[32, 33] (49% vs 15%). In contrast, promoters of stable genes overlap modENCODE High Occupancy Target (HOT) regions, associated to open chromatin and ubiquitous expression[34, 35], more often than promoters of regulated genes (67% vs. 8%). We also found that the overall pattern of transcription factor binding clearly separates regulated from stable genes, as revealed by Principal Component Analysis (PCA) based on ChIP-chip data for 20 transcription factors in fly embryos (Fig. 8a). Finally, analyses of published data[36-40] of knockdowns or overexpression of several transcription factors have frequently larger impact on the expression of regulated than of stable genes (Supplementary Table 8).

Regulated genes also exhibit a characteristic genome organization. We mapped our sets of stable and regulated genes to a number of genome segmentations, representing epigenomic domains, recently obtained in *Drosophila* cell lines (Kc167[41], BG3 and S2[42]) and developmental time points (late embryo, LE, and L3[43]). We systematically found that regulated genes tend to occur in chromatin states that are depleted in histone modifications (Figure 8b-d), even when considering only regulated genes expressed in the developmental time point at which the segmentation has been obtained (Figure 8b). Epigenomic domains in turn, spatially organize into well-defined physical domains within the nucleus[44]. Silent chromatin regions, in particular, fold into modular chromosomal entities, which we found enriched in regulated genes (Fig. 8e). The nuclear lamina plays a key role in this physical organization, through the interaction with large continuous chromosomal domains. These Lamina Associated Domains (LADs) are generally depleted of chromatin marks[45], and we consistently found that regulated genes are strongly enriched in LADs (52% compared to 5% of stable genes in 412 LADs from Kc167 cells[46]).

Histone modifications and alternative splicing

Beyond its role in primary RNA production, chromatin structure has also been implicated in subsequent steps of RNA processing. In particular, a number of studies have uncovered a relationship between nucleosome occupancy and exon-intron structure[47, 48] and between specific histone modifications and alternative splicing[49-51]. We found in fly WID and EID that highly included exons are characterized by higher H3 occupancy when compared to

lowly included ones, as previously reported in mammals[48] (Methods, Supplementary Tables 9, 10 and Supplementary Fig. 13a, b), and that the correlation between H3 occupancy and exon inclusion peaks very close to the acceptor site (Supplementary Fig. 13c, d).

We speculated, thus, that strong chromatin marking might not be only associated to more stable RNA production, but also to a tighter regulation of alternative splicing. To measure alternative splicing complexity, we computed the Shannon's entropy on the relative abundance of a gene's alternative splicing isoforms (Methods). The splicing entropy grows with the number of isoforms and with the evenness of their relative abundances. Higher entropic values can be interpreted as tight regulation of alternative splicing, while lower values would correspond to more stochastic production of alternative isoforms. As hypothesized, splicing entropy, measured at the time point of maximum gene expression, is lower for strongly marked stable genes than for unmarked developmentally regulated genes (Fig. 8f). Further supporting tighter regulation of splicing, we also found that the major isoform captures a larger fraction of the total transcriptional output in stable than in regulated genes (Fig. 8g).

Discussion

Cell type specific transcriptional regulation is crucial to maintain cell identity throughout the lifetime of organisms, yet it must be flexible enough to allow for responses to endogenous and exogenous stimuli. This regulation is mediated by specific molecular factors (e.g. cell type specific transcription factors, and chromatin modifications), as well as by the topological organization of the genome. In particular, modifications occurring on DNA and on histones regulate gene expression by establishing and maintaining specific chromatin states[52, 53]. The association of certain modifications with transcriptional activation or repression has become widely accepted. Nevertheless, expression of genes in the absence of chromatin marks has also been reported[6-9]. Here we found that transcription in the absence of most canonically active chromatin marks is actually a characteristic feature of genes that are regulated during fly and worm development. These are not necessarily equivalent to developmental control genes, many of which are known to be marked[11, 52].

Analyses of tissue-specific gene expression data, as well as our targeted validation experiments, support that our observations do not arise from the expression of developmentally regulated genes being low or confined to small cell populations, from limited detection sensitivity, and/or from persistence in the cell of RNA molecules transcribed at some earlier standpoint. Thus, while factors not accounted for cannot be completely ruled out, our observations appear to reflect a true biological property of genes regulated throughout development—maybe a consequence of these genes being partially unresponsive to histone modifications systems.

We also found that strongly marked chromatin state is associated to more tightly controlled transcriptional and post-transcriptional regulation, in particular to splicing. This is consistent with earlier observations[54] of simultaneous enrichment in the expression of chromatin modifying enzymes and splicing factors in cell-enriched testis, and with the higher levels of

H3K36me3 found by de Almeida et al.[49] in mammalian constitutive exons compared to alternative exons.

Overall, our results lead us to hypothesize that the relative contribution of transcription factors and histone modifications to regulation of gene expression differentiates the transcriptional programs of stable and regulated genes. In stable genes that are constitutively expressed, strong chromatin marking leads to transcriptional stability and tightly controlled RNA production. In these genes, regulation by transcription factors would play a comparatively smaller role. In contrast, genes regulated during development that need to be rapidly activated and de-activated are characterized by an unmarked chromatin state. In these other genes, transcription factors binding to chromatin would play the predominant regulatory role. These distinct regulatory programs would be reflected in the topological organization of the chromatin fiber within the nucleus, with regulated genes located in silent chromosomal modular domains that physically interact with the nuclear lamina[55].

While we found evidence for this model of transcriptional regulation specifically in the fly, preliminary results suggest that it may be generalizable to other metazoans. Although detailed transcriptional, epigenetic, and topological maps of genomes are being produced in an increasing number of cell lines and tissues, developmental maps are still sparse in mammalian species. Exhaustive monitoring through a much larger variety of conditions, differentiation states and developmental stages is required to fully understand the layer of epigenetic regulation that mediates between genome sequence and RNA production.

Online Methods

Drosophila strains

The strains used were: *Canton S* as a wild type and *nub*-GAL4/+; UAS-GFP/+. Flies were kept on standard media at 25°C.

Tissue disaggregation and cell sorting

Wing imaginal discs (WID) from *nub*-GAL4/+; UAS-GFP/+ flies were dissected in PBS and incubated for 1h in a 10x trypsin solution (Sigma T4174) at room temperature in a rotating wheel. Cells were vigorously pipetted and kept on ice in Schneider's insect medium. To discard dead cells, DAPI was added to the sample at 1 μg/mL final concentration. Cells were sorted in a FACSAria (BD) with the 85 μm nozzle. We were able to recover around $2.5 \cdot 10^6$ GFP negative and $2 \cdot 10^6$ GFP positive cells from 400 WIDs. An independent sorting experiment was done per each replicate, both for ChIPs and gene expression analyses.

RNA extraction, retrotranscription and Real-Time PCR

As starting material, 120 WID and 250 eye-antenna imaginal discs (EID) were used for RNASeq. For *pdm2* gene expression analysis, WIDs from 400 *nub*-GAL4/+; UAS-GFP/+ flies were disaggregated. RNA from sorted cells was extracted with ZR-RNA MicroPrep Kit from Zymo Research. For L3-specific genes expression, 5 third instar larvae were frozen and RNA was extracted with Quick-RNA MiniPrep Kit, from Zymo Research. Retrotranscriptions and qPCRs were performed as described previously[17]. For quantification

Europe PMC Funders Author Manuscripts

of RNA amounts, standard curves of each pair of primers were performed and the efficiency of amplification was calculated. The Cts obtained from the qPCR were corrected according to the amplification efficiency of the primers. Primers used for Real-Time PCR are listed in Supplementary Table 11.

Genetic mosaics

Clones mutant for *ash2*^{I1} were obtained by mitotic recombination using the *FLP/FRT* technique[57]. *yw;FRT82Bash2*^{I1}*/TM6C* flies were crossed with *ywhsflp;FRT82BGFP/TM6B* and wing and eye imaginal discs from third instar *Tubby*$^{+}$ larvae were dissected. Heat shock was carried out for 45 minutes at 37°C [52 ± 4 hours after egg laying (AEL)] to induce clone generation.

In situ hybridizations and immunohistochemistry

In situ hybridizations and immunostaining were carried out according to standard protocols. The cDNA for *pdm2* was PCR amplified using primers listed below and cloned into a pBSK +/− vector at *EcoR*I restriction site. Riboprobe was synthesized using T7 polymerase and digoxigenin labeled ribonucleotides (Roche). Alkaline phosphatase conjugated with anti-digoxigenin (Roche) and NBT and BCIP (Roche) were used to develop *in situ* hybridization. Peroxidase conjugated anti-digoxigenin and Tyramide signal amplification (TSA, Life Technologies) was used for fluorescent *in situ* hybridization (FISH). WIDs and EIDs were analyzed with a DMLB microscope and SPE confocal microscope (Leica). Primary antibodies used were: rabbit anti-H3K4me3 (1:1,000, Abcam/ab8580), mouse anti-En (1:25, DSHB/4D4) and mouse anti-CycA (1:100, DSHB/A12), mouse anti-BOSS (1:1,000)[58] and rabbit anti-GFP (1:1,000, Santa Cruz Biotechnology/sc-8334). Fluorescently labeled secondary antibodies were from Life Technologies and Jackson Immunochemicals. Discs were mounted in SlowFade (Life Technologies) supplemented with 1 μM TO-PRO-3 (Life Technologies) to label nuclei. For all *in situs* and immunostainings around 10 imaginal discs were analyzed. All experiments were performed twice.

Chromatin immunoprecipitation

Third instar larva WID or EID isolated from *Canton S* flies were fixed, pooled in 700 μL and processed as described[17]. Around 300 imaginal discs were used in these experiments. Trypsin treated cells from GFP transgenic flies were fixed after sorting for 10 minutes at room temperature and sonicated in a Diagenode Bioruptor for 15 minutes at high power in lysis buffer (1% SDS, 10 mM Tris HCl ph 8.0 and 2mM EDTA). Immunoprecipitations were performed in RIPA buffer. For L3 ChIPs and Imaginal Discs ChIPSeq experiments we used 1 μg of the corresponding antibody. For ChIPs in sorted cells we used 0.45 μg of anti-H3K4me3, 0.3 μg of anti-H3K36me3, 0.33 μg of anti-H3K27ac and 1 μg of anti-H3K27me3. For L3 time-specific ChIPs, 5 *Canton S* wall-wandering third instar larvae were disrupted, fixed and sonicated as indicated above. . Immunocomplexes were recovered with Invitrogen ProteinA magnetic beads for 2h. The beads were washed three times in RIPA or IP buffer, once in LiCl buffer and twice in TE[17]. Primers used for Real-Time PCR are listed in Supplementary Table 11. The antibodies used for ChIP were: H3 (Abcam/ab1791); H3K4me3 (Abcam/ab8580) (Millipore-Upstate/07-473), H3K9ac (Abcam/ab4441),

H3K36me3 (Abcam/ab9050), H3K4me1 (Diagenode/CS-037-100), H3K27ac (Abcam/ab4729) and H3K27me3 (Upstate-Millipore/07-449).

Nascent RNA

For Nascent RNA assays, 400 WIDs *nub*-GAL4/+; *UAS*-GFP/+ were dissected and disaggregated as described above. Click-IT® Nascent RNA Capture Kit from Molecular Probes (C10635) was used according to the manufacturer's instructions. Briefly, disaggregated cells were incubated with 0.5 mM 5-ethynil uridine (EU) in Schneider's Insect Medium for 1 h at room temperature. Total RNA was extracted and biotinylated with 0.25 mM biotin-azide for 30 minutes at room temperature. Biotinylated RNA was precipitated overnight at −80°C and purified with Streptavidin conjugated beads for 30 minutes at room temperature. Nascent RNA was eluted in 0.1 % SDS 5 minutes at 99°C and retrotranscription was carried out as described above. Four biological replicates were performed. Primers used for Real-Time PCR are listed in Supplementary Table 11.

Solexa/Illumina sequencing

Solexa/Illumina sequencing was carried out at the Ultrasequencing Unit of the Centre for Genomic Regulation (CRG, Barcelona, Spain). All protocols for Solexa/Illumina ChIPSeq and for RNASeq analysis were carried out following the manufacturer's protocol. For ChIPSeq, 10 ng of each sample were used and fragments between 300 and 350 bp were size selected before sequencing. For RNASeq, 5 μg of total RNA were used to sequence.

Drosophila melanogaster genome and annotation

We used the FlyBase[12] annotation release 5.12 for the genome version dm3.

RNASeq and ChIPSeq read mapping

Reads of 36 and 40 bp obtained from single-end RNASeq and ChIPSeq sequencing from WID and EID-cells were aligned using GEM[59] allowing up to two mismatches to the *D. melanogaster* genome (version dm3) and, for RNA, to all possible junctions of 5′-3′-ordered exon pairs occurring within the same annotated gene. ChIPSeq and RNASeq raw data and profiles of read counts were deposited in the NCBI-GEO repository under the accession number GSE56551.

Gene and transcript expression analysis

Reads mapping uniquely to the genome were used to quantify genes and transcripts separately in each tissue using the FluxCapacitor[60]. Expression levels are given in Reads Per Kilobase per Million mapped reads (RPKM). Linear regression analysis between log transformed WID and EID RPKMs gave a highly significant slope and intercept. Thus, we identified 628 genes at least one unit above the linear regression line (differentially expressed genes in EID) and 184 genes at least one unit below (differentially expressed genes in WID). To build our collection of regulated tissue-specific genes from each differentially expressed gene set, we required coefficient of variation >= 1.2 and at least 1.5 RPKMs in one tissue and less than 0.1 RPKM in the other one (55 EID-specific genes and 10 WID-specific genes, respectively, resulted from this criterion). Finally, those genes with

coefficient of variation < 1.2 that are expressed in both tissues (> 2.3 RPKMs) with a difference in expression of less than 20% were selected as stable expressed in the two tissues (284 genes) and the genes whose expression in both tissues is 0 RPKMs were considered to be silent (30 genes).

ChIPSeq analyses

ChIPSeq reads for H3, H3K4me3, H3K9ac, H3K36me3, H3K4me1 and H3K27ac were extended to the full average fragment length in the corresponding experiment. For each position in the genome the number of extended ChIPSeq reads overlapping this position was recorded. Each sample was normalized by the total number of sequenced reads and the average fragment length. The genome-wide correlation between WID and EID samples was computed using the UCSC Table browser on windows of 1,000 nucleotides[56]. To compute the correlation between ChIPSeq samples and RNASeq expression data, we assigned to each gene the highest peak of the corresponding ChIP signal within the gene body and correlated this value to the expression of the gene. To produce the graphical distribution of reads for each sample around a particular site (Transcription Start Sites, TSS, polyAdenylation Sites, pAS and splice Acceptor Sites, AS), we calculated the weighted number of reads on each position from −500 bp to +500bp of each TSS, pA and AS, according to FlyBase. To graphically represent an idealized gene, we normalized the location of the reads within the gene using a window of 100 units, and calculated the mean at each point. We extended this representation 500 bps upstream and downstream of the gene. To compare WID and EID samples, we calculated the weighted number of reads on each position in the normalized ChIPSeq profiles.

ENCODE and Roadmap Epigenomic analyses

Stable and developmentally regulated genes in *D. melanogaster*—To define the transcriptional stability of genes, we calculated the coefficient of variation of gene expression, as reported by the modENCODE consortium[10], for each protein-coding gene that has detectable expression in 12 selected developmental time points (Supplementary Fig. 1a). From the full ranking of 13,635 genes, we defined the bottom 1,000 genes with lowest variation of expression during development as stable, and the top 1,000 genes with highest variation as developmentally regulated genes. In addition, at each time point we selected the same number of silent genes than regulated genes expressed at that time point, for a total of 1,000 silent genes. For these genes, we measured the strength of the highest peak (measured as the log of the number of reads reported by modENCODE) within the gene body at the time point in which its expression is maximum for H3K4me3, H3K9ac, H3K4me1, H3K27ac, and the average signal within the gene body for H3K27me3 and H3K9me3 modENCODE ChIPSeq profiles (NCBI GEO accession: GSE16013). Due to data issues with ChIPSeq for three samples: H3K9ac (Adult male) and H3K9me3 (L3 and Adult male), we used ChIP-chip data in these cases instead. The Wilcoxon test (two-sided) was used to evaluate the statistical significance of the difference between ChIP values for stable, regulated and silent genes on each sample. To build the subsets of low, medium and high regulated genes, we ranked the top 1,000 regulated genes by their expression (in the time point of maximum expression) and we classified them into three groups of the same number of genes. Partial correlations between the coefficient of variation and the histone marking of

genes, with the effect of the expression of such genes removed, were calculated with the ggm R package.

L3-specific genes analysis

To compare the expression and histone modification marking levels in regulated broadly expressed and stable tissue-specific genes we used anatomy RNASeq data from modENCODE consortium available in Flybase[12]. We used the gene sets previously defined for modENCODE analysis to create new subgroups of genes:

- Stable: the 1,000 genes with the lowest coefficient of variation of gene expression across modENCODE time points
- Silent: genes identified as silent in L3 stage (RPKM = 0)
- Regulated broadly-expressed at L3: developmentally regulated genes that are detected in L3 whole body data, and that are furthermore expressed with at least 1 RPKM in each of the 6 tissues with L3 tissue-RNASeq available
- Stable tissue-specific at L3: from the set of extended stably expressed genes (P1 in Supplementary Fig 4) we selected the genes that, using L3 tissue-RNASeq, are detected as expressed with at least 10 RPKM in 1 of the tissues and not higher than 1 in all the other remaining tissues. We identified 26 carcass-specific genes, 8 central nervous system-specific genes, 36 digestive-specific genes, 21 fat body-specific genes, 36 imaginal disc-specific genes and 4 salivary glands-specific genes.

The expression and histone modification levels were calculated using L3 data from modENCODE following the methodology of the previous analysis.

Stable and developmentally regulated genes in *C. elegans*

We estimated H3K4me3 and H3K36me3 levels in 7 developmental stages (Early Embryo, Late Embryo, Larvae L1, L2, L3, L4 and Young Adult) from array signal files in Gerstein et al[35]. To define developmentally stable and regulated genes, we also used the same procedure as in fly. To obtain gene and transcript quantifications, we mapped the RNASeq reads from modENCODE *C. elegans*[35] to the Wbcel215.68 version of the genome using GEM[59], and used the FluxCapacitor[60] to produce the quantifications. Partial correlations between the coefficient of variation and the histone marking of genes, with the effect of the expression of such genes removed, were calculated with the ggm R package.

Human and mouse analyses

To define the transcriptional stability of human genes, we calculated the coefficient of variation of gene expression, as reported by the Roadmap Epigenomics Consortium, for each protein-coding gene that has detectable expression in the set of 56 consolidated epigenomes[14]. From the full ranking of 18,064 genes, we defined as constant genes the bottom 1,000 genes with lowest variation of expression across the 56 tissues and cell lines, and the top 1,000 genes with highest variation as variable genes. In addition, at each

epigenome we selected the same number of silent genes than variable genes expressed at that tissue, for a total of 1,000 silent genes. For these genes, we measured the strength of the highest peak (measured as the log of the number of reads reported by the Roadmap Epigenomics consortium) within the gene body at the tissue in which its expression is maximum for H3K4me3, H3K36me3 and H3K4me1. The Wilcoxon test (two-sided) was used to evaluate the statistical significance of the difference between ChIP values for constant, variable and silent genes on each sample. Partial correlations between the coefficient of variation and the histone marking of genes, with the effect of the expression of such genes removed, were calculated with the ggm R package.

The same protocol was applied in the analysis of the mouse ENCODE[15] RNASeq and ChIPSeq (H3K4me3, H3K9ac, H3K36me3, H3K4me1 and H3K27ac) data in ten adult tissues for which RNASeq data and ChIPSeq data all modifications are available: Cerebellum, Cortex, Heart, Kidney, Liver, Placenta, Small intestine, Spleen, Testis and Thymus.

Nucleosome turnover

Using the provided Nascent RNA signal tracks in S2 cells[18] with no treatment we calculated the average signal in the gene body of the previously defined stable, regulated and silent gene sets. Stable and regulated genes with signal over 1 were kept (986 stable and 56 regulated) and silent genes with signal equal 0 were also kept (258 genes). In these remaining genes we calculated the nucleosome turnover rate as the average CATCH-IT signal, within the gene body, in S2 cells with no treatment[18]. The Wilcoxon test (two-sided) was used to evaluate the statistical significance of the signal among the gene sets.

Promoter analyses

To measure the conservation of the promoters of regulated and stable genes across 12 Drosophilids, we computed the average of the UCSC PhastCons multiz15way track[56] along the promoter sequences of each gene set (promoter length: 200 bp). To characterize the promoters of regulated and stable genes, we used the MatScan program[61] with the full collection of 827 predictive matrices available in Jaspar and Transfac[62, 63]. From each initial pool of predictions, we removed those binding sites within genome regions in the UCSC genome browser that presented on average a probability lower than 0.95 to be conserved across the 12 flies PhastCons multiz15way alignments[64]. The Wilcoxon test (one-sided) was used to evaluate the statistical significance of the difference for stable and developmentally regulated gene sets on each comparison (PhastCons scores and number of conserved sites). For the identification of focused/dispersed initiation sites[8, 33], we searched for putative binding sites of TBP and DRE in the promoter sequence of the top 1,000 stable and the top 1,000 regulated genes (promoter length: 100 bp). We selected TBP as a marker of focused initiation and DRE as a representative of dispersed initiation. The weight matrix for TBP is from Jaspar[62] and for DRE is from Fly Factor Survey[65].

Principal Components Analysis (PCA) was performed based on the ChIPSeq levels of 20 Transcription Factors in Embryos at 0–12h in the promoter regions of genes with expression above 10 as measured by tilling arrays at this time point[6].

Genome segmentations

To match the states of a particular map of genome segmentation and our sets of stable and regulated genes, we counted how many genes of these two groups overlap with the segments of each state. To annotate our collection of genes, we used the modENCODE ChromHMM[66] maps of BG3 and S2 cell lines[42], the hiHMM maps of Late Embryo and L3[43] and the chromatin types identified by Filion and colleagues[41]. To annotate the topological information of stable and regulated genes, we conducted a 4similar analysis on the HiC genome domains previously identified on Late Embryo[44] and the Lamina Associated Domains reported in Kc cells[46].

Trancription factor perturbation analysis

To study the effects of transcription factors in stable and regulated genes we analyzed publicly available data on knock-down or overexpression of various *Drosophila* transcription factors[36-40]. First we checked how many stable and regulated genes were expressed in the tissue/cell type used in each study before the perturbation of the transcription factor, using published expression data on brain L3[36], Kc cells[67], S2 cells[67] and our L3 eye imaginal disc. Genes with RPKM > 1 were considered expressed. Then, we intersected the stable and regulated expressed genes with the genes identified as differentially expressed in each study.

Splicing entropy

For each gene, we computed the Shannon's entropy (or diversity index) based on the relative frequencies of the gene's annotated isoforms in a given cell line. Let g be a gene with n annotated isoforms with relative frequencies $p_1, \ldots, p_n$, in a given condition, the entropy of g, $H(g)$, is computed as

$$H(g) = -\sum_{i=1}^{n} p_i \log p_i$$

$H(g)$ growths with the number of annotated isoforms and with the evenness of their frequencies. $H(g)$ is zero when there is only one expressed isoform (which would correspond to tight regulation of isoform expression), and it is maximum when all isoforms are equally expressed (which would correspond to lack of splicing regulation and stochastic production of alternative splicing isoforms). Based on transcript quantifications produced by the modENCODE project for the fly, and computed by us for the worm (see Methods), we calculated the splicing entropy of each gene at the developmental time point in which its expression is at its maximum. The boxplots in Figure 8f display the distribution of $H(g)$, separately for genes with different number of isoforms.

Supplementary Material

Refer to Web version on PubMed Central for supplementary material.

Acknowledgements

We thank D. Gonzalez-Knowles, A. Breschi and M. Melé, for help with data analysis, F. Serras, M. Morey and A. Kornblihtt for insightful suggestions and G. Cavalli for discussing data before publication, as well as the

anonymous reviewers for their critical input. We thank the modENCODE, ENCODE (human and mouse) and the Roadmap Epigenomics Mapping consortiums for granting open access of these resources to the scientific community. We also thank the Ultrasequencing Unit of the CRG (Barcelona, Spain), for sample processing and the Confocal Unit of the CCiTUB (Universitat de Barcelona, Spain). This work was performed under the financial support of the Spanish Ministry of Economy and Competitiveness with grants BIO2011-26205 to RG, CSD2007-00008 and BFU2012-36888 to M. C., and 'Centro de Excelencia Severo Ochoa 2013-2017', SEV-2012-0208, and of the ERC/European Community PF7 with grant 294653 RNA-MAPS to R. G. E. B. is supported by the European Commission's 7th Framework Program 4DCellFate grant number 277899. This research reflects only the authors' views and that the Community is not liable for any use that may be made of the information contained therein. J. C. is supported by grant SFRH/BD/33535/2008 from the Portuguese Foundation to Science and Technology.

References

1. Li B, Carey M, Workman JL. The role of chromatin during transcription. Cell. 2007; 128:707–19. [PubMed: 17320508]
2. Black JC, Van Rechem C, Whetstine JR. Histone lysine methylation dynamics: establishment, regulation, and biological impact. Mol Cell. 2012; 48:491–507. [PubMed: 23200123]
3. Wagner EJ, Carpenter PB. Understanding the language of Lys36 methylation at histone H3. Nat Rev Mol Cell Biol. 2012; 13:115–26. [PubMed: 22266761]
4. Dong X, et al. Modeling gene expression using chromatin features in various cellular contexts. Genome Biol. 2012; 13:R53. [PubMed: 22950368]
5. Karlic R, Chung HR, Lasserre J, Vlahovicek K, Vingron M. Histone modification levels are predictive for gene expression. Proc Natl Acad Sci U S A. 2010; 107:2926–31. [PubMed: 20133639]
6. Negre N, et al. A cis-regulatory map of the Drosophila genome. Nature. 2011; 471:527–31. [PubMed: 21430782]
7. Hodl M, Basler K. Transcription in the absence of histone H3.2 and H3K4 methylation. Curr Biol. 2012; 22:2253–7. [PubMed: 23142044]
8. Chen K, et al. A global change in RNA polymerase II pausing during the Drosophila midblastula transition. Elife. 2013; 2:e00861. [PubMed: 23951546]
9. Zhang H, Gao L, Anandhakumar J, Gross DS. Uncoupling transcription from covalent histone modification. PLoS Genet. 2014; 10:e1004202. [PubMed: 24722509]
10. Graveley BR, et al. The developmental transcriptome of Drosophila melanogaster. Nature. 2011; 471:473–9. [PubMed: 21179090]
11. Roy S, et al. Identification of functional elements and regulatory circuits by Drosophila modENCODE. Science. 2010; 330:1787–97. [PubMed: 21177974]
12. Tweedie S, et al. FlyBase: enhancing Drosophila Gene Ontology annotations. Nucleic Acids Res. 2009; 37:D555–9. [PubMed: 18948289]
13. Spencer WC, et al. A spatial and temporal map of C. elegans gene expression. Genome Res. 2011; 21:325–41. [PubMed: 21177967]
14. Kundaje A, et al. Integrative analysis of 111 reference human epigenomes. Nature. 2015; 518:317–30. [PubMed: 25693563]
15. Yue F, et al. A comparative encyclopedia of DNA elements in the mouse genome. Nature. 2014; 515:355–64. [PubMed: 25409824]
16. Barski A, et al. High-resolution profiling of histone methylations in the human genome. Cell. 2007; 129:823–37. [PubMed: 17512414]
17. Perez-Lluch S, et al. Genome-wide chromatin occupancy analysis reveals a role for ASH2 in transcriptional pausing. Nucleic Acids Res. 2011; 39:4628–39. [PubMed: 21310711]
18. Teves SS, Henikoff S. Transcription-generated torsional stress destabilizes nucleosomes. Nat Struct Mol Biol. 2014; 21:88–94. [PubMed: 24317489]
19. Luque CM, Milan M. Growth control in the proliferative region of the Drosophila eye-head primordium: the elbow-noc gene complex. Dev Biol. 2007; 301:327–39. [PubMed: 17014842]

20. Weihe U, Dorfman R, Wernet MF, Cohen SM, Milan M. Proximodistal subdivision of Drosophila legs and wings: the elbow-no ocelli gene complex. Development. 2004; 131:767–74. [PubMed: 14757638]
21. Ng M, Diaz-Benjumea FJ, Cohen SM. Nubbin encodes a POU-domain protein required for proximal-distal patterning in the Drosophila wing. Development. 1995; 121:589–99. [PubMed: 7768195]
22. Beltran S, Angulo M, Pignatelli M, Serras F, Corominas M. Functional dissection of the ash2 and ash1 transcriptomes provides insights into the transcriptional basis of wing phenotypes and reveals conserved protein interactions. Genome Biol. 2007; 8:R67. [PubMed: 17466076]
23. Beltran S, et al. Transcriptional network controlled by the trithorax-group gene ash2 in Drosophila melanogaster. Proc Natl Acad Sci U S A. 2003; 100:3293–8. [PubMed: 12626737]
24. Zeitlinger J, Stark A. Developmental gene regulation in the era of genomics. Dev Biol. 2010; 339:230–9. [PubMed: 20045679]
25. Stark A, et al. Discovery of functional elements in 12 Drosophila genomes using evolutionary signatures. Nature. 2007; 450:219–32. [PubMed: 17994088]
26. Carninci P, et al. Genome-wide analysis of mammalian promoter architecture and evolution. Nat Genet. 2006; 38:626–35. [PubMed: 16645617]
27. Gaertner B, et al. Poised RNA polymerase II changes over developmental time and prepares genes for future expression. Cell Rep. 2012; 2:1670–83. [PubMed: 23260668]
28. Hoskins RA, et al. Genome-wide analysis of promoter architecture in Drosophila melanogaster. Genome Res. 2011; 21:182–92. [PubMed: 21177961]
29. Rach EA, Yuan HY, Majoros WH, Tomancak P, Ohler U. Motif composition, conservation and condition-specificity of single and alternative transcription start sites in the Drosophila genome. Genome Biol. 2009; 10:R73. [PubMed: 19589141]
30. Ni T, et al. A paired-end sequencing strategy to map the complex landscape of transcription initiation. Nat Methods. 2010; 7:521–7. [PubMed: 20495556]
31. Lenhard B, Sandelin A, Carninci P. Metazoan promoters: emerging characteristics and insights into transcriptional regulation. Nat Rev Genet. 2012; 13:233–45. [PubMed: 22392219]
32. Teves SS, Henikoff S. The heat shock response: A case study of chromatin dynamics in gene regulation. Biochem Cell Biol. 2013; 91:42–8. [PubMed: 23442140]
33. Juven-Gershon T, Kadonaga JT. Regulation of gene expression via the core promoter and the basal transcriptional machinery. Dev Biol. 2010; 339:225–9. [PubMed: 19682982]
34. Farley E, Levine M. HOT DNAs: a novel class of developmental enhancers. Genes Dev. 2012; 26:873–6. [PubMed: 22549952]
35. Gerstein MB, et al. Integrative analysis of the Caenorhabditis elegans genome by the modENCODE project. Science. 2010; 330:1775–87. [PubMed: 21177976]
36. Froldi F, et al. The transcription factor Nerfin-1 prevents reversion of neurons into neural stem cells. Genes Dev. 2015; 29:129–43. [PubMed: 25593306]
37. Georlette D, et al. Genomic profiling and expression studies reveal both positive and negative activities for the Drosophila Myb MuvB/dREAM complex in proliferating cells. Genes Dev. 2007; 21:2880–96. [PubMed: 17978103]
38. Pennington KL, Marr SK, Chirn GW, Marr MT 2nd. Holo-TFIID controls the magnitude of a transcription burst and fine-tuning of transcription. Proc Natl Acad Sci U S A. 2013; 110:7678–83. [PubMed: 23610421]
39. Pineyro D, Blanch M, Badal M, Kosoy A, Bernues J. GAGA factor repression of transcription is a rare event but the negative regulation of Trl is conserved in Drosophila species. Biochim Biophys Acta. 2013; 1829:1056–65. [PubMed: 23860261]
40. Turkel N, et al. The BTB-zinc finger transcription factor abrupt acts as an epithelial oncogene in Drosophila melanogaster through maintaining a progenitor-like cell state. PLoS Genet. 2013; 9:e1003627. [PubMed: 23874226]
41. Filion GJ, et al. Systematic protein location mapping reveals five principal chromatin types in Drosophila cells. Cell. 2010; 143:212–24. [PubMed: 20888037]

42. Kharchenko PV, et al. Comprehensive analysis of the chromatin landscape in Drosophila melanogaster. Nature. 2011; 471:480–5. [PubMed: 21179089]
43. Ho JW, et al. Comparative analysis of metazoan chromatin organization. Nature. 2014; 512:449–52. [PubMed: 25164756]
44. Sexton T, et al. Three-dimensional folding and functional organization principles of the Drosophila genome. Cell. 2012; 148:458–72. [PubMed: 22265598]
45. Guelen L, et al. Domain organization of human chromosomes revealed by mapping of nuclear lamina interactions. Nature. 2008; 453:948–51. [PubMed: 18463634]
46. van Bemmel JG, et al. The insulator protein SU(HW) fine-tunes nuclear lamina interactions of the Drosophila genome. PLoS One. 2010; 5:e15013. [PubMed: 21124834]
47. Schwartz S, Meshorer E, Ast G. Chromatin organization marks exon-intron structure. Nat Struct Mol Biol. 2009; 16:990–5. [PubMed: 19684600]
48. Tilgner H, et al. Nucleosome positioning as a determinant of exon recognition. Nat Struct Mol Biol. 2009; 16:996–1001. [PubMed: 19684599]
49. de Almeida SF, et al. Splicing enhances recruitment of methyltransferase HYPB/Setd2 and methylation of histone H3 Lys36. Nat Struct Mol Biol. 2011; 18:977–83. [PubMed: 21792193]
50. Luco RF, et al. Regulation of alternative splicing by histone modifications. Science. 2010; 327:996–1000. [PubMed: 20133523]
51. Sims RJ 3rd, et al. Recognition of trimethylated histone H3 lysine 4 facilitates the recruitment of transcription postinitiation factors and pre-mRNA splicing. Mol Cell. 2007; 28:665–76. [PubMed: 18042460]
52. Delest A, Sexton T, Cavalli G. Polycomb: a paradigm for genome organization from one to three dimensions. Curr Opin Cell Biol. 2012; 24:405–14. [PubMed: 22336329]
53. Espada J, Esteller M. DNA methylation and the functional organization of the nuclear compartment. Semin Cell Dev Biol. 2010; 21:238–46. [PubMed: 19892028]
54. Gan Q, et al. Dynamic regulation of alternative splicing and chromatin structure in Drosophila gonads revealed by RNA-seq. Cell Res. 2010; 20:763–83. [PubMed: 20440302]
55. Ciabrelli F, Cavalli G. Chromatin-driven behavior of topologically associating domains. J Mol Biol. 2015; 427:608–25. [PubMed: 25280896]
56. Karolchik D, et al. The UCSC Genome Browser Database: 2008 update. Nucleic Acids Res. 2008; 36:D773–9. [PubMed: 18086701]

References of online methods

57. Xu T, Rubin GM. Analysis of genetic mosaics in developing and adult Drosophila tissues. Development. 1993; 117:1223–37. [PubMed: 8404527]
58. Cagan RL, Kramer H, Hart AC, Zipursky SL. The bride of sevenless and sevenless interaction: internalization of a transmembrane ligand. Cell. 1992; 69:393–9. [PubMed: 1316239]
59. Derrien T, et al. Fast computation and applications of genome mappability. PLoS One. 2012; 7:e30377. [PubMed: 22276185]
60. Montgomery SB, et al. Transcriptome genetics using second generation sequencing in a Caucasian population. Nature. 2010; 464:773–7. [PubMed: 20220756]
61. Blanco E, Messeguer X, Smith TF, Guigo R. Transcription factor map alignment of promoter regions. PLoS Comput Biol. 2006; 2:e49. [PubMed: 16733547]
62. Portales-Casamar E, et al. JASPAR 2010: the greatly expanded open-access database of transcription factor binding profiles. Nucleic Acids Res. 2010; 38:D105–10. [PubMed: 19906716]
63. Wingender E. The TRANSFAC project as an example of framework technology that supports the analysis of genomic regulation. Brief Bioinform. 2008; 9:326–32. [PubMed: 18436575]
64. Siepel A, et al. Evolutionarily conserved elements in vertebrate, insect, worm, and yeast genomes. Genome Res. 2005; 15:1034–50. [PubMed: 16024819]
65. Zhu LJ, et al. FlyFactorSurvey: a database of Drosophila transcription factor binding specificities determined using the bacterial one-hybrid system. Nucleic Acids Res. 2011; 39:D111–7. [PubMed: 21097781]

66. Ernst J, Kellis M. ChromHMM: automating chromatin-state discovery and characterization. Nat Methods. 2012; 9:215–6. [PubMed: 22373907]

67. Cherbas L, et al. The transcriptional diversity of 25 Drosophila cell lines. Genome Res. 2011; 21:301–14. [PubMed: 21177962]

Europe PMC Funders Author Manuscripts

Europe PMC Funders Author Manuscripts

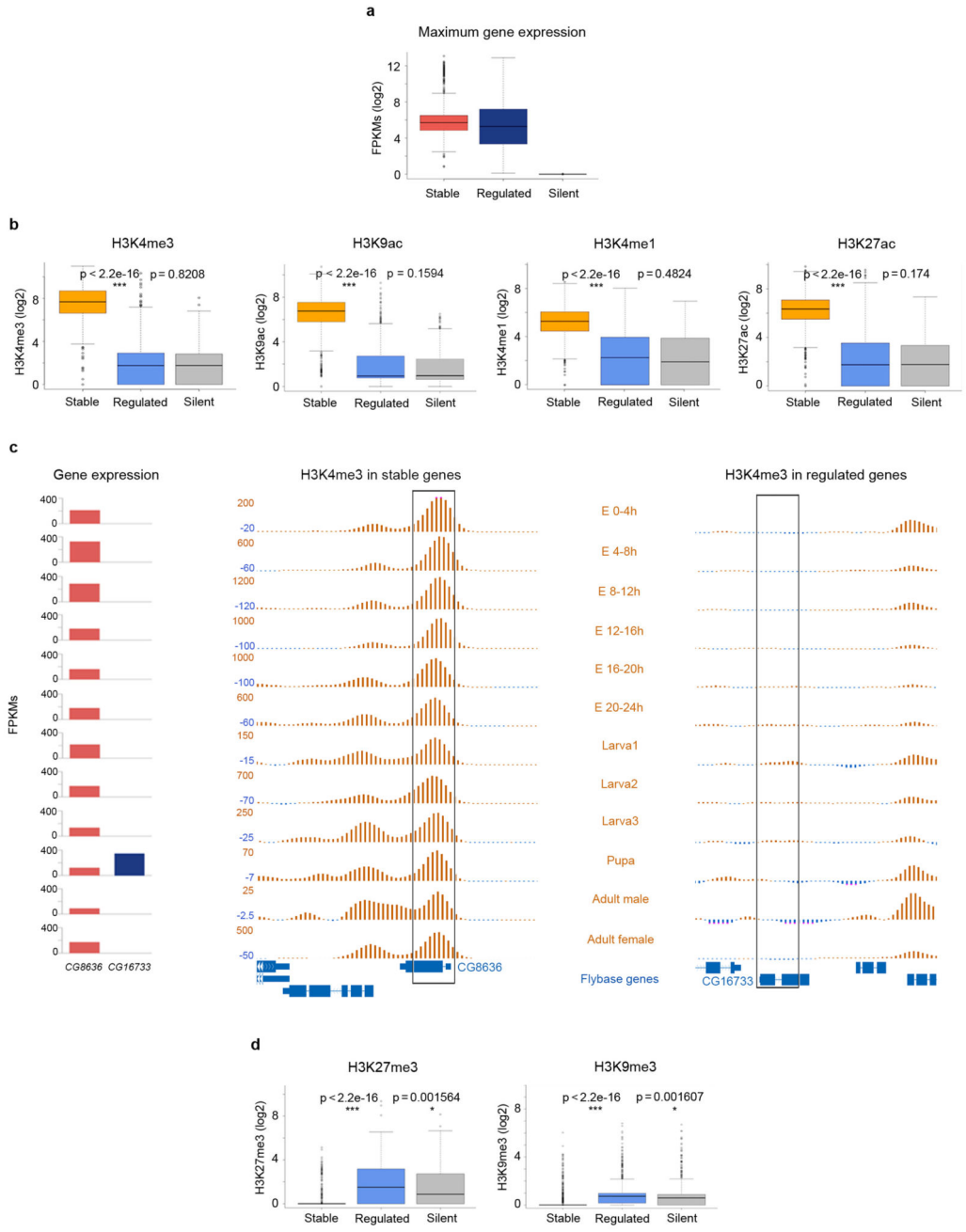

Figure 1. Distribution of histone modification levels in stable, regulated and silent genes during fly development

a, Expression of stable, regulated, and silent genes during fly development at the time point of maximum expression for each gene. Gene expression was computed as FPKMs by the modENCODE consortium. The bottom and top of the boxes are the first and third quartiles, and the line within, the median. The whiskers denote the interval within 1.5 times the Inter Quartile Range (IQR) from the median. Outliers are plotted as dots. **b,** Normalized levels of H3K4me3, H3K9ac, H3K4me1 and H3K27ac at the time point of maximum expression

during *D. melanogaster* development. These values represent the maximum height of the ChIPSeq peak within the gene body. P-values were computed using the Wilcoxon text (two-sided). **c**, Profiles of H3K4me3 during the 12 fly developmental time points in *CG8636*, a gene stably expressed during fly development, and *CG16733*, a pupa-specific gene. The expression (measured as FPKMs) along these points for the two genes is given on the left. **d**, Levels of H3K27me3 and H3K9me3 at the time point of maximum expression, computed as the average height of the ChIPSeq signal within the gene body, in stable, regulated and silent genes.

Europe PMC Funders Author Manuscripts

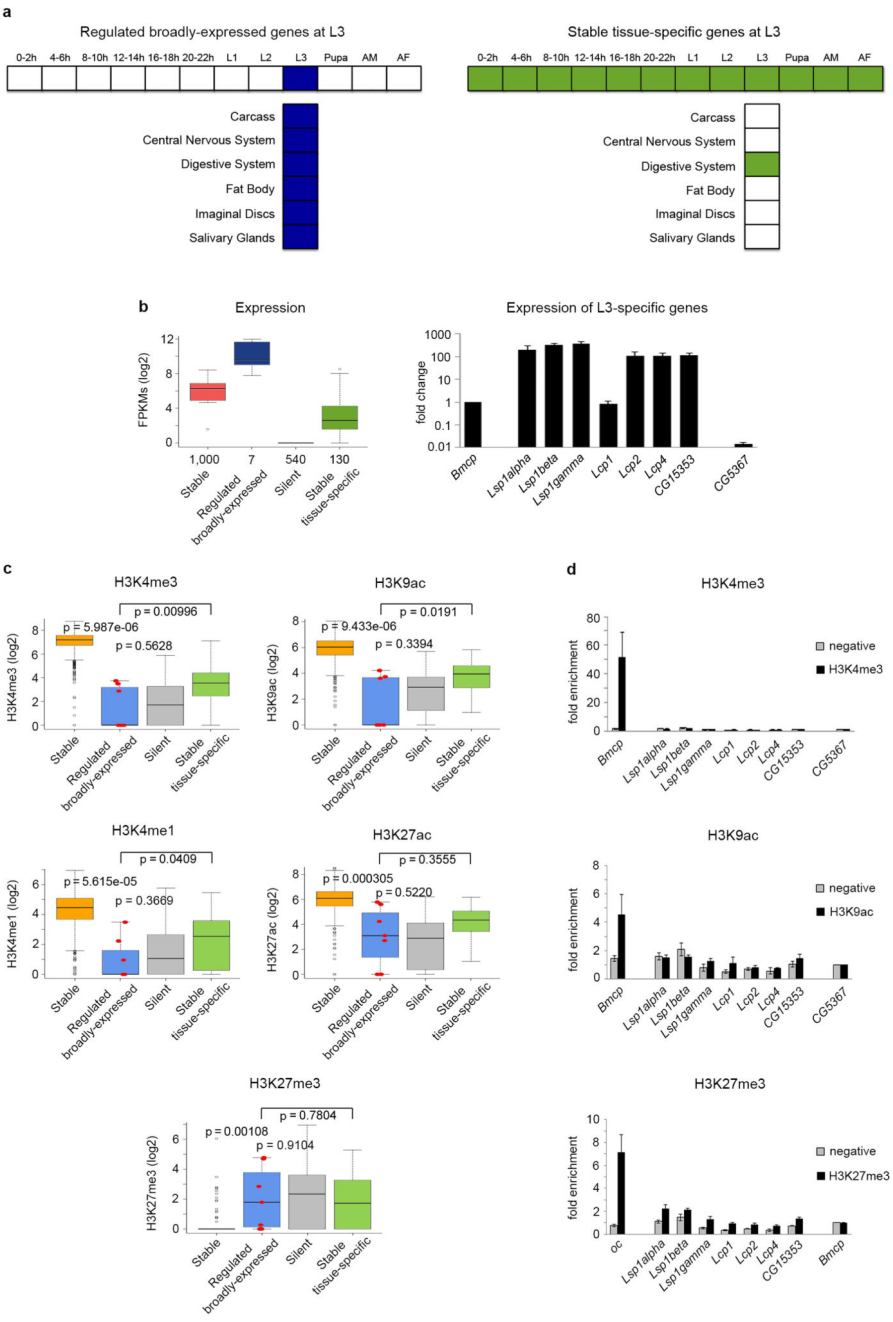

Figure 2. Gene expression and histone modifications in regulated broadly-expressed and stable tissue-specific genes at third instar larvae

a, Diagrams of developmentally regulated genes broadly-expressed across multiple tissues at third instar-larvae L3 (left panel), and stable genes expressed in only one tissue at L3 (right panel). **b,** Gene expression levels at L3 measured by whole organism RNASeq (left panel). The number of genes in each category is given under the boxplots. The bottom and top of the boxes are the first and third quartiles, and the line within, the median. The whiskers denote the interval within 1.5 times the IQR from the median. Outliers are plotted as dots.

Europe PMC Funders Author Manuscripts

Validation by qPCR of the expression at L3 of regulated broadly-expressed genes compared to a stable gene (*Bmcp*) and a silent gene (*CG5367*) (right panel). Error bars represent the Standard Error of the Mean (SEM) from three independent replicates. **c,** Levels of H3K4me3, H3K9ac, H3K4me1 and H3K27ac on whole L3 individuals. The seven regulated genes broadly-expressed at L3 are depicted as red dots within the boxplots. P-values were computed using the Wilcoxon test (two-sided). **d,** Validation by individual ChIPs and qPCR of H3K4me3 and H3K9ac in regulated genes broadly-expressed at L3. H3K4me3 and H3K9ac ChIPs are represented as enrichment of the marks over the silent gene (*CG5367*). Error bars represent the SEM from three independent replicates.

Europe PMC Funders Author Manuscripts

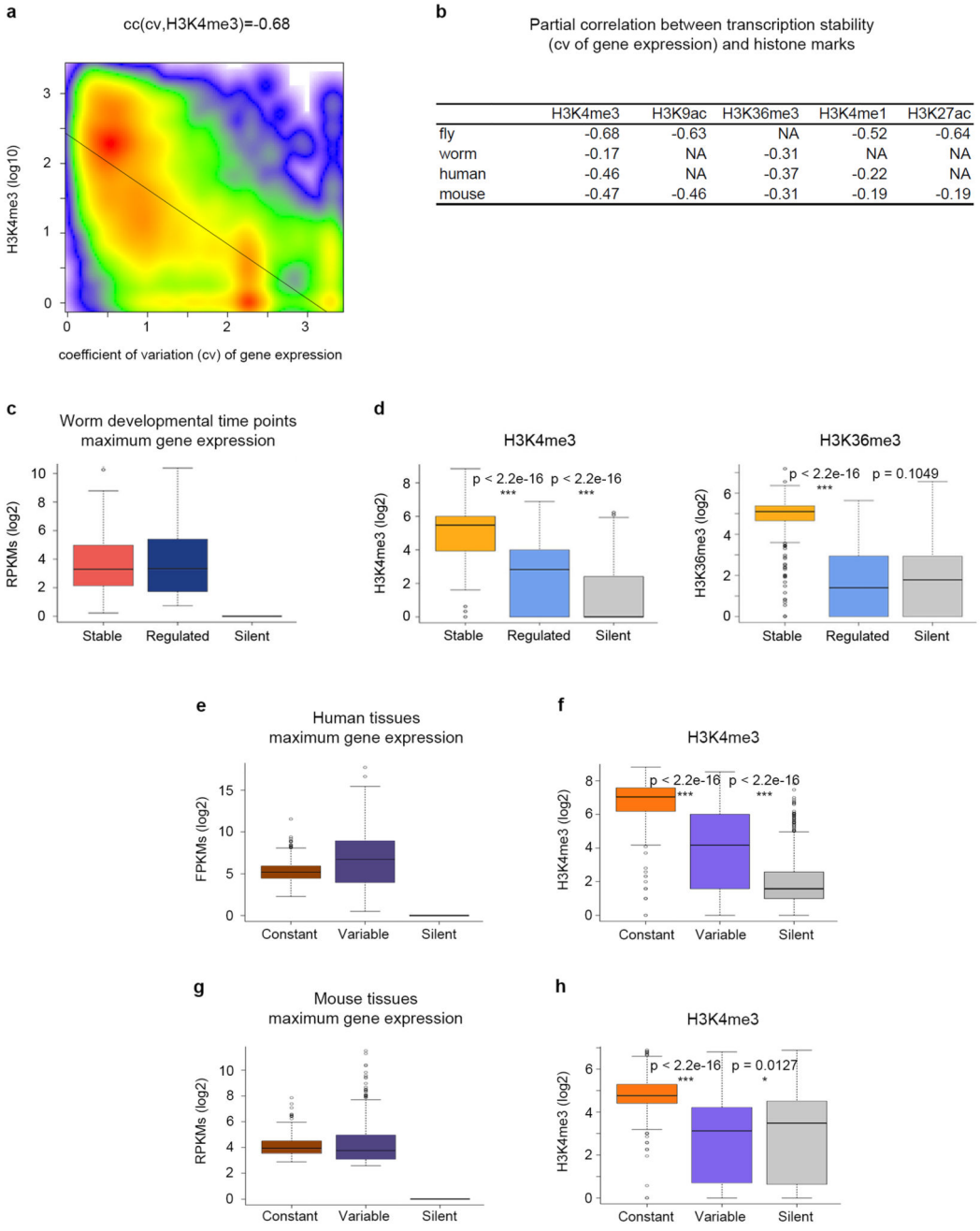

	H3K4me3	H3K9ac	H3K36me3	H3K4me1	H3K27ac
fly	-0.68	-0.63	NA	-0.52	-0.64
worm	-0.17	NA	-0.31	NA	NA
human	-0.46	NA	-0.37	-0.22	NA
mouse	-0.47	-0.46	-0.31	-0.19	-0.19

Figure 3. Association between histone modifications and transcription stability in metazoans

a, Scatterplot of H3K4me3 levels at the time point of highest expression during fly development and transcriptional stability measured as the coefficient of variation of gene expression across time points. The correlation is computed as the partial correlation given gene expression. **b,** Partial correlations between active marks and transcription stability (the coefficient of variation). Correlations are computed controlling for gene expression. All correlations are statistically significant (p-value < 2.2e–16). P-values were computed using Student's t-test (two-sided). **c,** Expression of stable, regulated and silent genes during worm

development at the time point of maximum expression. The bottom and top of the boxes are the first and third quartiles, and the line within, the median. The whiskers denote the interval within 1.5 times the IQR from the median. Outliers are plotted as dots. **d,** Levels of H3K4me3 and H3K36me3 at the time point of maximum expression during worm development. **e,** Expression of genes with constant and variable expression at the tissue/cell line of highest expression across multiple samples from the Roadmap Epigenomics Mapping Consortium. **f,** Levels of H3K4me3 at the tissue of maximum expression. **g,** Expression of genes with constant and variable expression at the tissue of highest expression across ten mouse tissues from the mouse ENCODE project. **h,** Levels of H3K4me3 at the tissue of maximum expression. These levels correspond to the maximum height of the ChIPSeq peak within the gene body. P-values were computed using Wilcoxon text (two-sided).

Europe PMC Funders Author Manuscripts

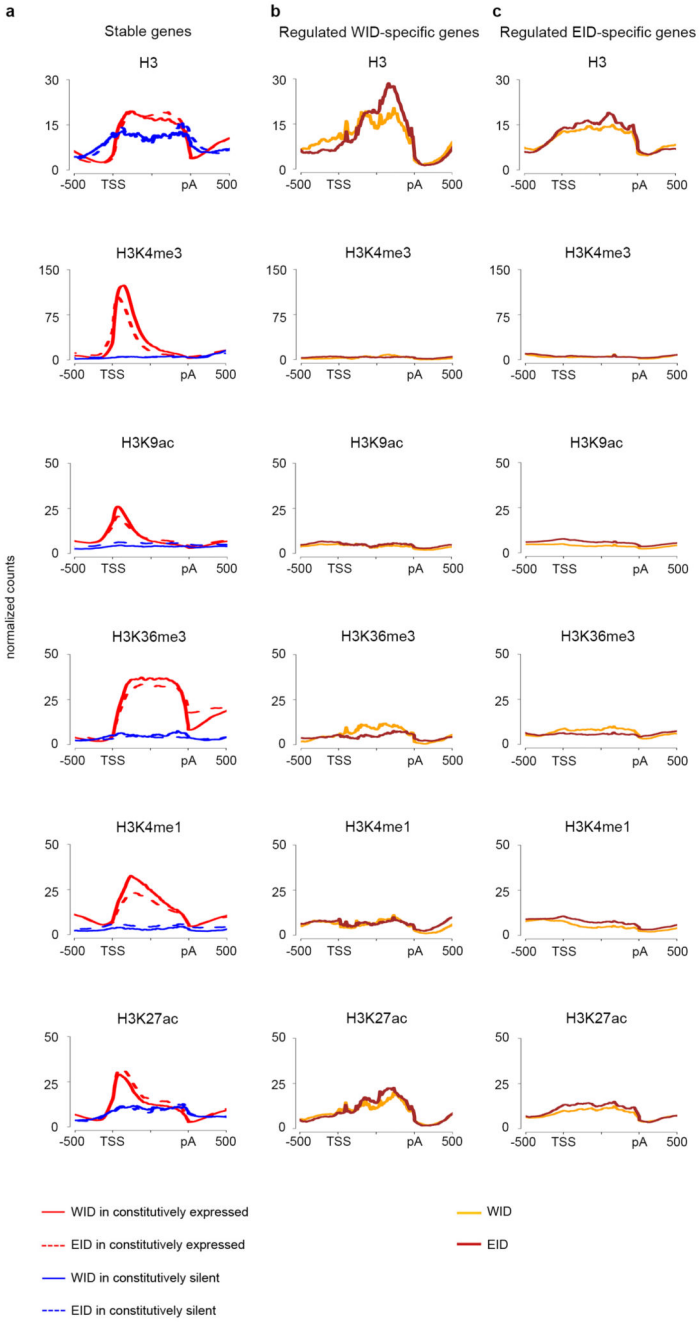

Figure 4. Profiles of H3 and histone modifications in Wing (WID) and Eye-antenna (EID) imaginal discs

a, Profiles on stable and silent genes in WID and in EID. **b**, Profiles on regulated WID-specific genes in WID and EID. **c,** Profiles on regulated EID-specific genes in WID and EID.

Europe PMC Funders Author Manuscripts

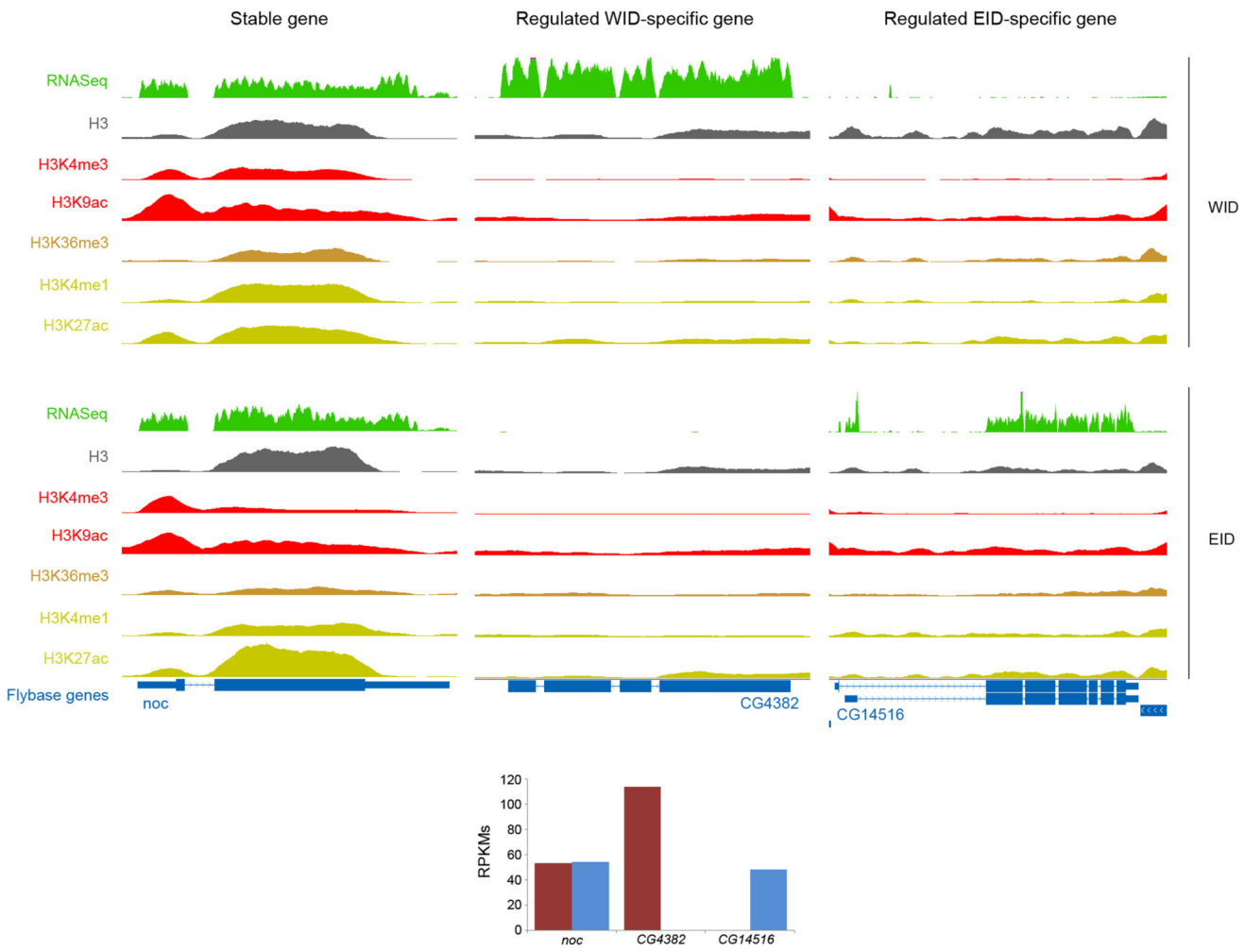

Figure 5. Profiles of RNA expression, H3 and histone modifications in Wing (WID) and Eye-antenna (EID) imaginal discs

Noc is a gene stably expressed in WID and EID; *CG4382* a WID-specific and *CG14516*, an EID-specific gene. Levels of gene expression (as RPKMs) are depicted at the bottom of the panels. Screenshots have been obtained through the UCSC Genome Browser[56].

Europe PMC Funders Author Manuscripts

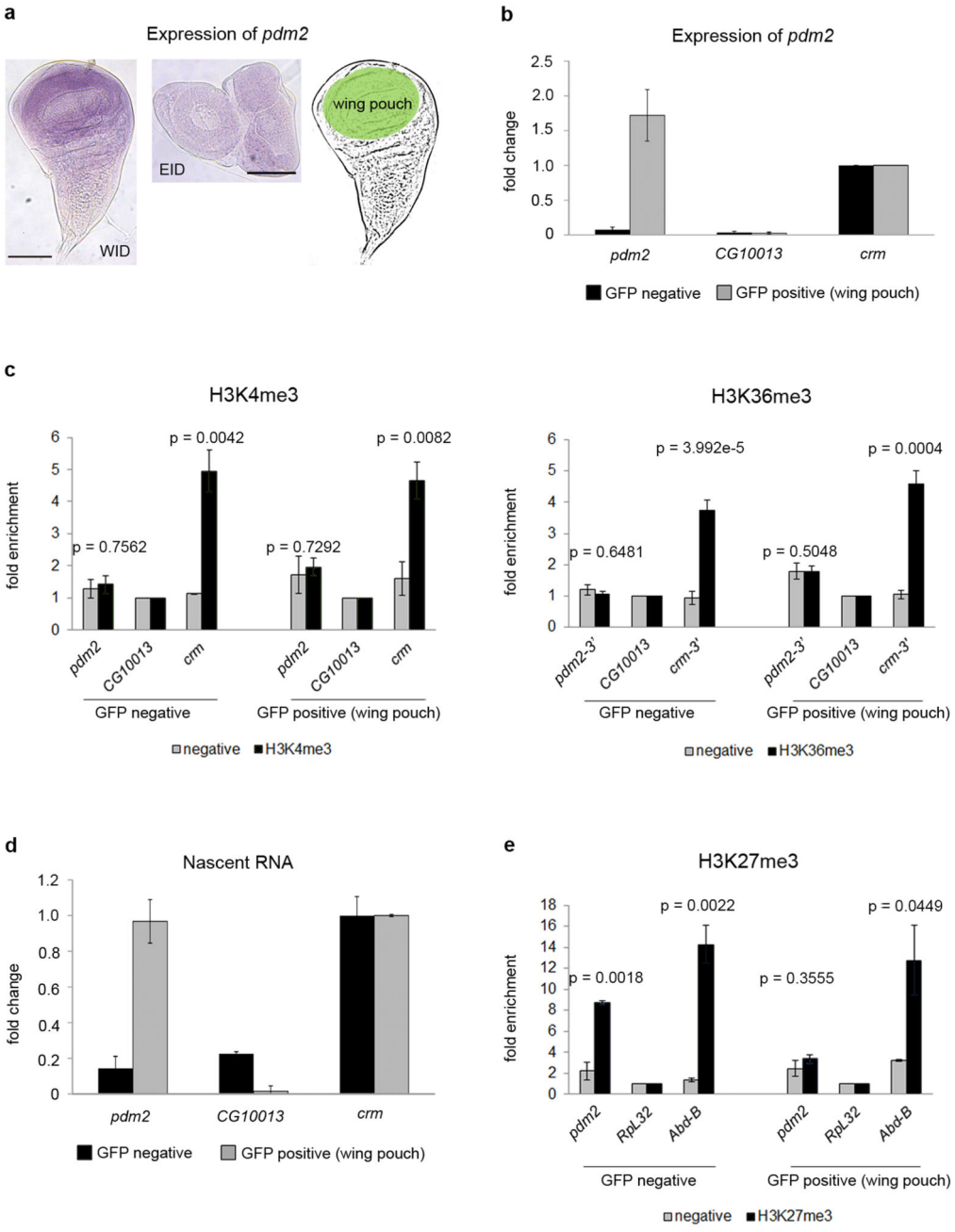

Figure 6. Active transcription of *pdm2* without chromatin modifications

a, Expression of *pdm2* in WID (left panel) and EID (middle panel) labeled with a *pdm2*-specific probe. The gene is only expressed in the wing pouch of the WID, highlighted in green. The scale bars represent 100 μm. **b,** Expression of *pdm2* in sorted cells analyzed by qPCR. Gene expression is normalized by the control gene *crm*. Error bars represent the SEM from three biological replicates. **c**, ChIP analysis of H3K4me3, H3K36me3 and of negative controls without antibody on sorted cells. ChIPs are represented as enrichment of the marks over a silent gene non-marked with H3K4me3 and H3K36me3 (*CG10013*). *Crm* is used as

positive control for these modifications. Error bars represent the SEM from at least three biological replicates. P-values were computed using the Student's t-test (two-sided). **d**, Newly transcribed RNA of GFP-sorted cells. Nascent RNA is normalized by the control gene *crm*. Error bars represent the SEM of four biological replicates. **e,** ChIP analysis of H3K27me3 and of negative controls without antibody on sorted cells. H3K27me3 ChIPs are represented as enrichment of the mark over a constitutively expressed gene non-marked with H3K27me3 (*RpL32*). *Abd-B* is used as positive control for this modification. Error bars represent the SEM from at least three biological replicates.

Europe PMC Funders Author Manuscripts

Europe PMC Funders Author Manuscripts

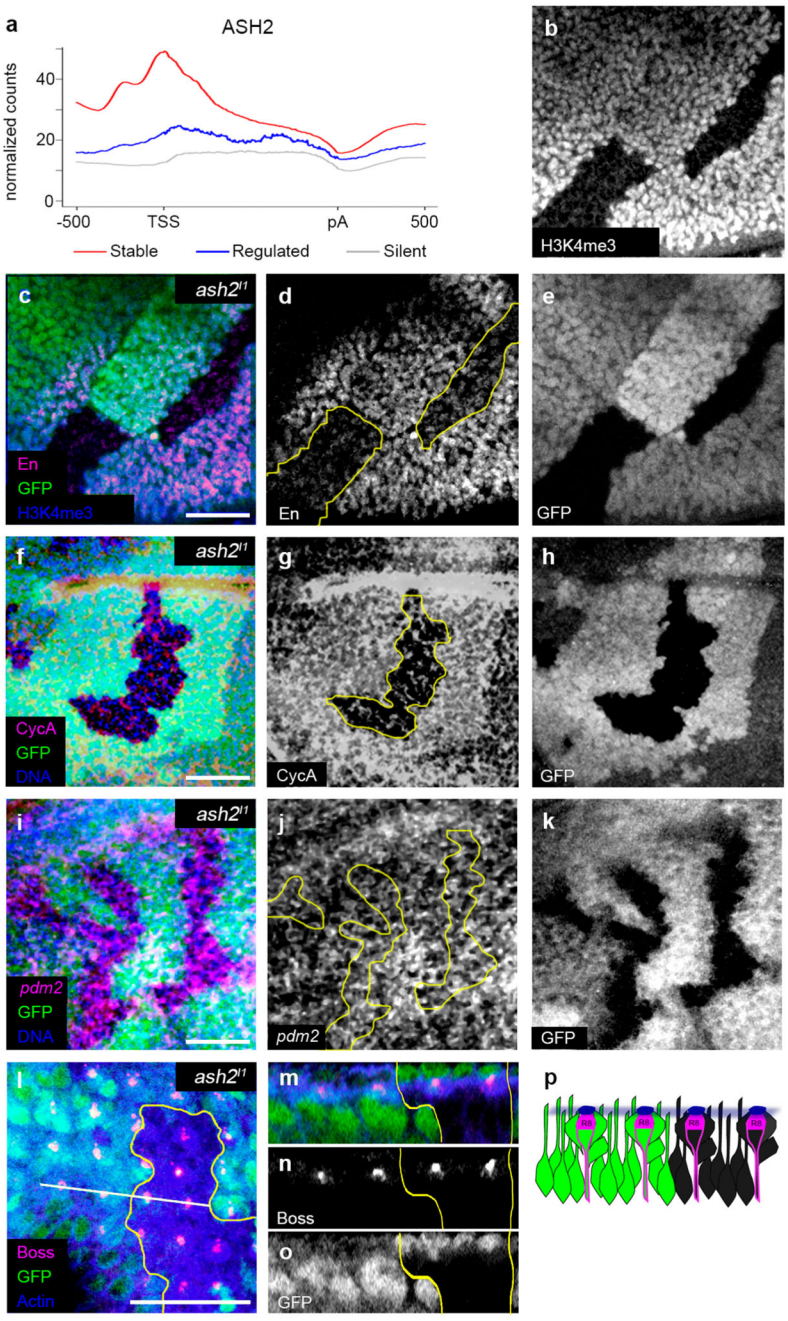

Figure 7. Reduction of H3K4me3 does not affect expression of regulated genes

a, Distribution of ASH2 binding in stable (red), regulated (blue) and silent genes (grey). **b**, H3K4me3 is strongly decreased in *ash2*^{I1} mutant clones in WID. **c**, En immunostaining in WID (merged). The scale bar represents 20 μm. **d**, The levels of the stable gene En are reduced in mutant clones. **e,** GFP negative cells indicate *ash2*^{I1} mutant cells in **c** and **d**. **f**, CycA immunostaining in WID (merged). The scale bar represents 20 μm. **g,** CycA is decreased in *ash2*^{I1} mutant clones. **h,** GFP negative cells indicate *ash2*^{I1} mutant cells in **f** and **g**. **i,** *pdm2* fluorescence *in situ* hybridization in *ash2*^{I1} mutant clones in WID (merged). The

scale bar represents 20 μm. **j**, No changes in *pdm2* expression are observed in *ash2*^{I1} mutant clones. **k,** GFP negative cells indicate *ash2*^{I1} mutant cells in **i** and **j**. **l,** Boss immunostaining in EID. The scale bar represents 20 μm. **m,** Optical cross-section (white line in **l**) showing Boss in all R8 photoreceptor cells (merged). **n**, No changes in Boss expression are observed in *ash2*^{I1} mutant clones. **o,** GFP negative cells indicate *ash2*^{I1} mutant cells in **m** and **n**. **p**, Diagram summarizing the result in **m**–**o**. Green cells express the wild-type *ash2* allele and black cells correspond to homozygous *ash2*^{I1} mutant cells. Boss (magenta cap) localizes in the apical side of R8.

Europe PMC Funders Author Manuscripts

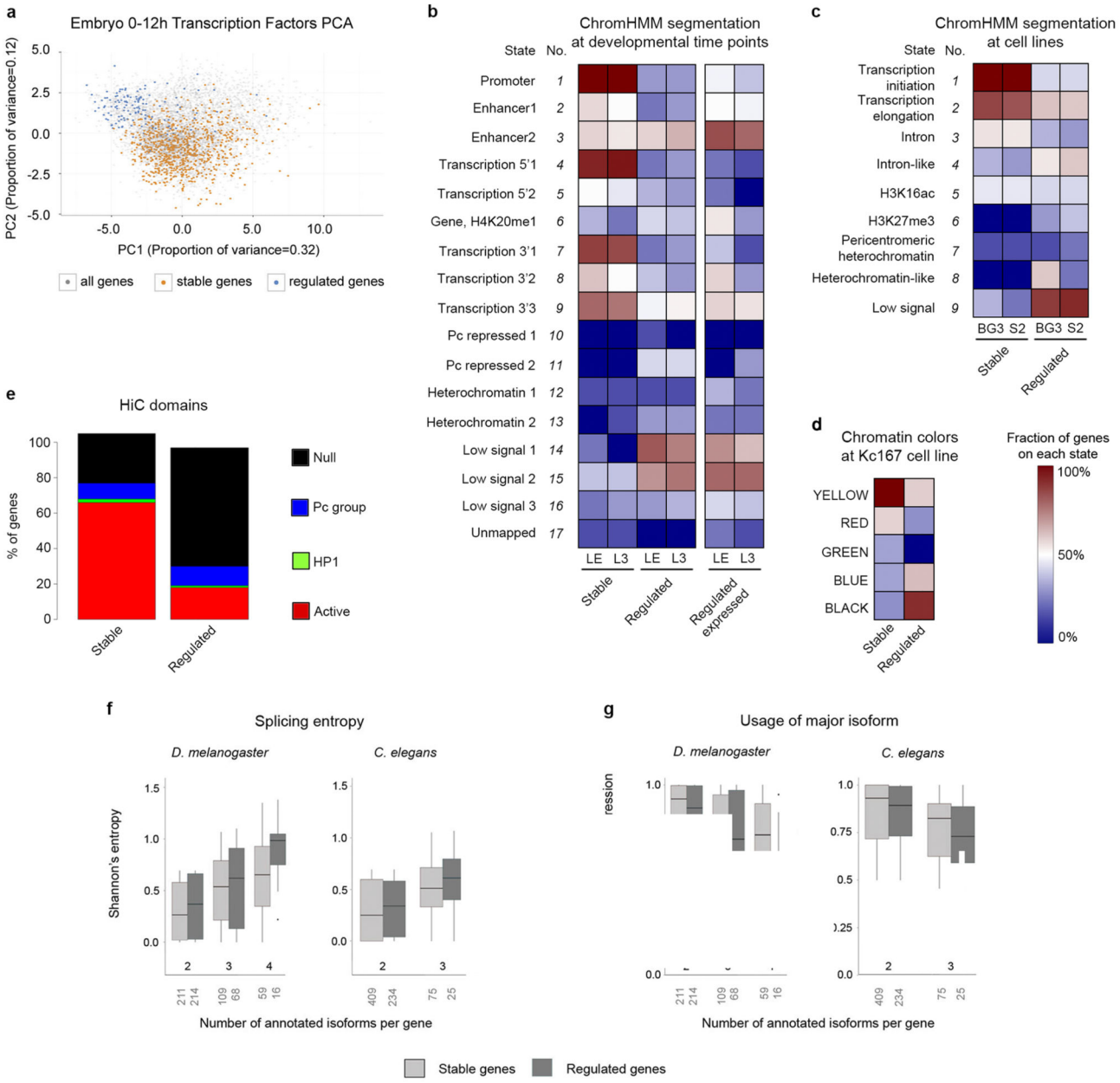

Figure 8. Promoter architecture and genome organization in stable and developmentally regulated genes

a, Principal Component Analysis (PCA) of genes expressed in the *Drosophila* embryo between 0 and 12h, based on ChIP-chip binding profiles of twenty transcription factors. **b,** Fraction of stable and regulated genes in different states from chromatin segmentations in Late Embryo (LE) and L3[43]. Right, proportion of regulated genes when considering only genes expressed in LE or L3. **c,** The same as in **b**, for segmentations in BG3 and S2 cell lines[42]. **d,** The same as in **b**, for the segmentation in Kc167[41]. BLACK chromatin corresponds to repressive chromatin. YELLOW and RED chromatin is typical of

Europe PMC Funders Author Manuscripts

transcriptionally active regions. GREEN and BLUE chromatin correspond to repressive chromatin. **e**, Proportion of stable and regulated genes mapping to spatial chromatin domains, considering the 1,169 domains inferred by HiC in fly embryos[44]. **f**, Distribution of Shannon's entropy of splicing in stable and regulated genes. Shannon's entropy is computed at the developmental time point in which gene expression is the maximum. The number of genes of each category appears below the X-axis. The bottom and top of the boxes are the first and third quartiles, and the line within, the median. The whiskers denote the interval within 1.5 times the IQR from the median. Outliers are plotted as dots. **g**, Distribution of the relative usage of the major isoform. The Y-axis is the fraction of the total transcriptional output of the gene that is captured by the most abundant isoform.

Europe PMC Funders Author Manuscripts